Digestive Diseases and Sciences (2019) 64:1815–1829
https://doi.org/10.1007/s10620-019-05496-8

ORIGINAL ARTICLE

Blockage of the P2X7 Receptor Attenuates Harmful Changes Produced by Ischemia and Reperfusion in the Myenteric Plexus

Kelly Palombit[1,2] · Cristina Eusébio Mendes[1] · Wothan Tavares-de-Lima[3] · Maria Luiza Barreto-Chaves[1] · Patricia Castelucci[1]

Received: 15 December 2017 / Accepted: 24 January 2019 / Published online: 7 February 2019

Abstract

Introduction Our work analyzed the effects of a P2X7 receptor antagonist, Brilliant Blue G (BBG), on rat ileum myenteric plexus following ischemia and reperfusion (ISR) induced by 45 min of ileal artery occlusion with an atraumatic vascular clamp with 24 h (ISR 24-h group) or 14 d of reperfusion (ISR 14-d group).

Material and methods Either BBG (50 mg/kg or 100 mg/kg, BBG50 or BBG100 groups) or saline (vehicle) was administered subcutaneously 1 h after ischemia in the ISR 24-h group or once daily for the 5 d after ischemia in the ISR 14-d group ($n = 5$ per group). We evaluated the neuronal density and profile area by examining the number of neutrophils in the intestinal layers, protein expression levels of the P2X7 receptor, intestinal motility and immunoreactivity for the P2X7 receptor, nitric oxide synthase, neurofilament-200, and choline acetyl transferase in myenteric neurons.

Results The neuronal density and profile area were restored by BBG following ISR. The ischemic groups showed alterations in P2X7 receptor protein expression and the number of neutrophils in the intestine and decreased intestinal motility, all of which were recovered by BBG treatment.

Conclusion We concluded that ISR morphologically and functionally affected the intestine and that its effects were reversed by BBG treatment, suggesting the P2X7 receptor as a therapeutic target.

Keywords P2X7 receptor · Brilliant Blue G · Myenteric plexus · Ischemia and reperfusion · Ileum

Introduction

The enteric nervous system (ENS) innervates the gastrointestinal tract and contains the myenteric plexus, whose functions include motility and the movement of fluid through the epithelium, and submucosal plexus, responsible for changes in local blood flow [1, 2].

The gut is affected by ischemia and reperfusion (ISR), which is most commonly caused by venous or arterial mesenteric thrombosis, embolism, or obstruction [3–5] and can also affect enteric neurons [6–10].

Adenosine 5′-triphosphate (ATP) is a transmitter in the nervous system and a signaling molecule that mediates many biological processes [11] and has been identified to activate P2 receptors [12–14]. P2 receptors are divided into ion channel-forming P2X receptors and G protein-coupled P2Y receptors [15]. P2X receptors are found in smooth muscle cells, glial cells, and neurons and have a mediating role in excitatory neurotransmission [16–18]. High levels of ATP are released upon cell damage or degeneration, particularly under traumatic or ischemic conditions [19, 20]. Additionally, P2X receptors have been identified in the ENS of guinea pigs [21–26], rats [27, 28], and mice [29, 30].

The P2X7 receptor forms a large pore after prolonged or repeated exposure to high levels of ATP [20, 31] and is associated with apoptosis, proliferation, and cell inflammation [32]. This receptor is widely expressed by enteric neurons, and its expression changes in response to colitis, ISR, and undernourishment [8, 33–35]. Neurons respond to

✉ Patricia Castelucci
pcastel@usp.br

[1] Department of Anatomy, Institute of Biomedical Sciences, University of São Paulo, Av. Prof. Dr. Lineu Prestes, 2415, São Paulo CEP 05508-900, Brazil

[2] Department of Morphology, Federal University of Piaui, Teresina, Brazil

[3] Department of Pharmacology, Institute of Biomedical Sciences, University of São Paulo, São Paulo, Brazil

ATP with an increase in intracellular calcium, followed by neuronal death, which can be prevented by P2X7 receptor antagonists [36, 37]. One such P2X7 receptor antagonist, a dye called Brilliant Blue G (BBG), blocks the activation of this receptor [38, 39].

Recent studies have demonstrated that administration of BBG prevents neuronal loss in an Alzheimer's disease model [40] and in a Huntington's disease mouse model [41]. A spinal cord injury study showed that intravenously administered BBG improved recovery and reduced local inflammation in rats [42]. Additionally, studies have demonstrated reduced brain damage following ischemia after treatment with a P2X7 antagonist [43, 44].

Here, we report the protective effects of a P2X7 receptor antagonist, BBG, in enteric neurons after intestinal ISR using several techniques, including immunohistochemistry, Western blotting, histology, and examination of intestinal motility.

Materials and Methods

The animal experiments in this study were conducted according to the current regulations of the Ethics Committee on Animal Use of the Biomedical Science Institute of the University of São Paulo. Furthermore, all protocols were approved by the Ethics Committee on Animal Use of the Biomedical Science Institute of the University of São Paulo (Protocol 126/10). Young male Wistar rats (200–300 g body weight) were maintained under standard conditions at 21 °C with a 12-h light–dark cycle. All groups were supplied with water ad libitum.

Induction of Ischemia

Forty rats were anesthetized with a subcutaneously administered mixture of xylazine (20 mg/kg) and ketamine hydrochloride (100 mg/kg). A loop of the distal ileum was exposed, and the ileal artery was located and occluded for 45 min with an atraumatic microsurgical vascular clamp (VASCU-STATT). Intestinal reperfusion was reestablished by clip release [7]. In the sham (SH) group, ten rats were subjected to identical manipulations but without arterial occlusion. The animals were weighed and then euthanized in a CO_2 chamber 24 h or 14 d after ischemia. Brilliant Blue G (BBG, 50 or 100 mg/kg, Sigma-Aldrich, UK) or saline was injected 1 h following reperfusion in the 24-h and 14-d groups and once daily for the 5 d after ischemia in the 14-d group [42]. The ileum was removed and washed in phosphate-buffered saline (PBS; 0.15 M NaCl in 0.01 M sodium phosphate buffer, pH 7.2). For immunofluorescence, five rat ilea per group were analyzed from the ISR group, the ISR group treated with 50 mg/kg BBG (BBG50 group), the ISR group treated with 100 mg/kg BBG (BBG100 group), and the SH-operated group (SH group). A total of 8 groups were included in the study as follows: SH 24 h, ISR 24 h, BBG50 24 h, BBG100 24 h, SH 14 d, ISR 14 d, BBG50 14 d, and BBG100 14 d. BBG and saline were given subcutaneously.

Immunohistochemistry

Forty ileal segments were dissected, cleaned with PBS, pinned mucosal side down onto a balsa wood board, and fixed overnight at 4 °C with 4% paraformaldehyde in 0.2 M sodium phosphate buffer (pH 7.3). Tissue collection was performed by the same researcher to maintain the same degree of stretch between preparations. Next, the tissue was washed 3 times for 10 min each in 100% dimethyl sulfoxide (DMSO) followed by 3 10-min washes in PBS and stored at 4 °C in PBS containing sodium azide (0.1%). Then, the tissue was dissected to produce longitudinal muscle-myenteric plexus whole mounts.

Myenteric plexus tissue was collected from 5 rats per group. A total of 80 whole-mount preparations were used per double-labeling assay. The tissues were incubated in 10% normal horse serum in PBS containing 1.5% Triton X-100 for 45 min at room temperature to reduce nonspecific binding and permeabilize the tissue. The antibodies and their combinations used for double labeling are described in Table 1. Following incubation in the primary antisera, the tissue was washed in PBS three times for 10 min each and incubated with various secondary antibodies (Table 1). The PBS washes were repeated, and the tissue was mounted in glycerol buffered with 0.5 M sodium carbonate (pH 8.6). The preparations were examined on a Nikon 80i fluorescence microscope, and images were captured using a digital camera and Image Pro Plus software version 4.1.0.0. Additionally, preparations were analyzed using confocal microscopy on a Zeiss confocal scanning laser system installed on a Zeiss Axioplan 2 microscope. Confocal images were

Table 1 Characteristics of primary and secondary antibodies

Antigen	Host	Dilution	Source
P2X7 receptor	Rabbit	1:200	Chemicon
NOS	Sheep	1:2000	EMSO
NF-200	Mouse	1:500	Sigma
ChAT	Goat	1:50	Chemicon
Anti-HuC/D	Mouse	1:100	Molecular probes
Secondary antibodies			
Donkey anti-rabbit IgG 488		1:500	Molecular probes
Donkey anti-sheep IgG 594		1:100	Molecular probes
Donkey anti-mouse IgG 594		1:200	Molecular probes
Donkey anti-sheep IgG 488		1:100	Molecular probes

collected using Zeiss LSM 5 image processing software and further processed using Corel Draw software.

Quantitative Analyses

For colocalization studies, neurons were identified by immunofluorescence. Labeling for the second antigen was evaluated using a second filter, allowing calculation of the proportion of neurons labeled for antigen pairs. For each group, data were collected from two preparations obtained from five animals and from 100 neurons per animal. The percentages of double-positive neurons were calculated and are expressed as the mean ± standard error (SEM). The neurons per area immunoreactive (ir) (neurons/cm^2) for the P2X7 receptor, neuronal nitric oxide synthase (nNOS), neurofilament-200 (NF200), and choline acetyl transferase (ChAT) were measured using two whole-mount preparations from 5 rats for each group. A total of eighty whole-mount preparations were used per immunoreactivity assay. Counts were made in 40 microscopic fields (0.000379 cm^2) chosen at random for each antigen in each animal, and a total of 200 microscopic fields were analyzed per immunoreactivity. Cell profile areas (μm^2) were obtained for 100 randomly selected neurons in two whole-mount preparations per animal per immunoreactivity assay from 5 rats for each group. A total of 500 neurons per group were analyzed using a Nikon 80i microscope coupled to a camera with NIS-Elements AR 3.1 (Nikon) software and were measured using Image Pro Plus software version 4.1.0.0.

Myeloperoxidase Reaction

Tissue samples (1 cm) were collected either 24 h or 14 d after ischemia from 5 rats in each group (40 rats total). The myeloperoxidase (MPO) reaction was performed as previously published [34]. Then, the tissues were cut with a cryostat (12-µm-thick slices) and mounted, with 3 slides per animal for each group. The tissues were stained for 10 min in Hanker-Yates (*p*-phenylenediamine more pyrocatechol; Polysciences, Warrington, Pennsylvania, USA) solution consisting of 0.6 mg/ml Hanker-Yates reagent and 0.003% H_2O_2 in PBS. The tissues were washed in PBS (3 × 5 min) and counterstained with 2% methyl green for 30 min. A total of 120 slides were analyzed. Qualitative and quantitative analyses of the neutrophil locations in the submucosal plexus and lamina propria, the longitudinal muscle, and the circular muscle of the ileum were performed for all groups. The neutrophils localized by using the MPO reaction were counted in the submucosal submucosa + intestinal glands and longitudinal and circular muscles. Those observed in the villi were not counted due to the early loss of villi that occurred during ISR.

Western Blotting

To evaluate the expression of the gut P2X7 receptor, total protein was obtained from the distal ileum, which was dissected to obtain the myenteric plexus + longitudinal layer, from 5 rats per group (40 rats total). A total of 40 experiments were performed to evaluate the expression of the P2X7 receptor, and the experiment was repeated twice. An extraction buffer (3 M KCl, 1 M *N*-2-hydroxyethylpiperazine-*N*′-2-ethanesulfonic acid, 1 M $MgCl_2$, 0.5 M ethylenediaminetetraacetic acid, 10% glycerol, 1 M dithiothreitol, 10% sodium dodecyl sulfate) was used to obtain protein from the tissues. The samples were separated by 10% sodium dodecyl sulfate polyacrylamide gel electrophoresis (SDS-PAGE) using a Bio-Rad mini-gel apparatus, and the fractionated protein on the gel was transferred to a membrane, which was incubated with primary antibodies against the P2X7 receptor (Chemicon) and β-actin (Santa Cruz Biotechnology, Santa Cruz, CA, USA, Sc47778). The membrane was probed with peroxidase-conjugated anti-rabbit and anti-goat immunoglobulin G secondary antibodies (Amersham Biosciences, Piscataway, NJ, USA). Signals were detected with enhanced chemiluminescence detection reagents (Amersham Biosciences) and exposure to X-ray film. The protein bands were quantified by densitometry and expressed as percentage of variation in relation to sham group. P2X7 receptor protein levels were normalized to α-actin levels.

Intestinal Motility

Full-thickness ileal segments (2 cm long) were used. Segments from 5 rats in each group (40 rats total) were prepared and mounted longitudinally in 20-ml organ baths containing Krebs' physiological saline. The baths were aerated with 95% O_2/5% CO_2 and maintained at 37 °C. A resting tension of 1 g was applied to the tissues, and isometric responses were recorded with a force transducer and displayed using AcqKnowledge 4 software (BIOPAC Systems, Inc., USA). Tissues were allowed to equilibrate for at least 60 min, and amplitude response curves were obtained before the addition of drugs, including carbachol (10 µM; Sigma-Aldrich) and sodium nitroprusside (SNP; 100 µM; Sigma-Aldrich). The addition of SNP to the organ bath inhibited spontaneous contractions, and the effect of SNP was measured by contraction. A total of 40 segments were analyzed. Before starting the experiments, the viability of each preparation was demonstrated by testing its contractility response to acetylcholine.

Statistical Analyses

Data were compared using analysis of variance (ANOVA) and Tukey's test for multiple comparisons. The data are

reported as the mean ± SEM. $P < 0.05$ was considered indicative of statistical significance.

Results

Qualitative Analysis

The P2X7 receptor was present throughout the cytoplasm and on the surface membranes of the nerve cells of the myenteric plexus in the SH, ISR, and BBG 24-h and 14-d animals (Figs. 1, 2, 3). P2X7 receptor-ir neurons were labeled for nNOS, NF200, and ChAT in all groups studied (Figs. 1, 2, 3). nNOS-ir neurons exhibited Dogiel type I morphology, and NF200-ir neurons exhibited Dogiel type II morphology (Figs. 1, 2).

Myeloperoxidase Reaction

The MPO reaction was used to reveal neutrophils in the ileum in all groups. In SH animals, no neutrophils were detected in the longitudinal muscle, enteric neurons, or circular muscle. In the ISR 24-h and 14-d groups, neutrophils were present in the muscle layers, mucosa, and lamina propria (LP) (Fig. 4a–h). In the submucosal plexus (SP) + LP layers, the number of neutrophils in the ISR 24-h group increased by 28%, 40%, and 34% compared with those in the SH, BBG50, and BBG100 groups, respectively. In the 14-d group, ISR increased the number of neutrophils by 38%, 20%, and 15% compared with those in the SH, BBG50, and BBG100 groups, respectively ($P < 0.001$) (Fig. 4i).

In the longitudinal muscle (LM) layer, the number of neutrophils in the 24-h I/R, BBG50, and BBG100 groups increased by 190%, 160%, and 250%, respectively, compared with that in the sham group. In the 14-d groups, the number of neutrophils in the I/R, BBG50, and BBG100 groups increased by 200%, 130%, and 170%, respectively, compared with that in the sham group ($P < 0.001$) (Fig. 4j).

Additionally, neutrophils appeared to be present in the muscularis propria in the SH group and following ISR and were reduced by BBG treatment (Fig. 4j).

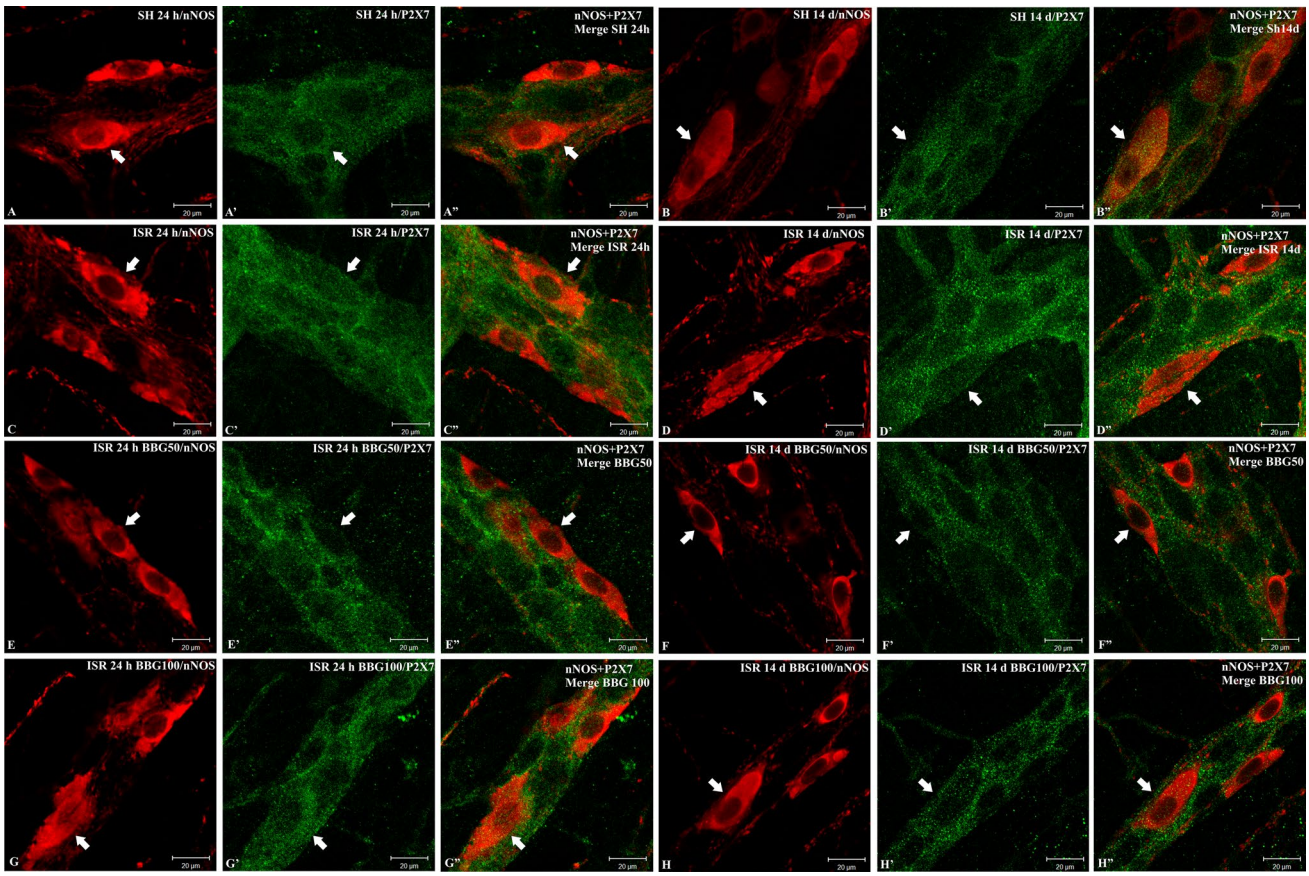

Fig. 1 Double labeling of the P2X7 receptor (P2X7) and neuronal nitric oxide synthase (nNOS) in rat ileum myenteric plexus from the SH, ISR, BBG50, and BBG100 groups at 24 h and 14 d. NOS (red; **a–h**) colocalized with the P2X7 receptor (green; **a′–h′**). Merge of the P2X7 receptor and NOS (**a″–h″**). Single arrows indicate double-labeled neurons. Scale bars, 20 µm

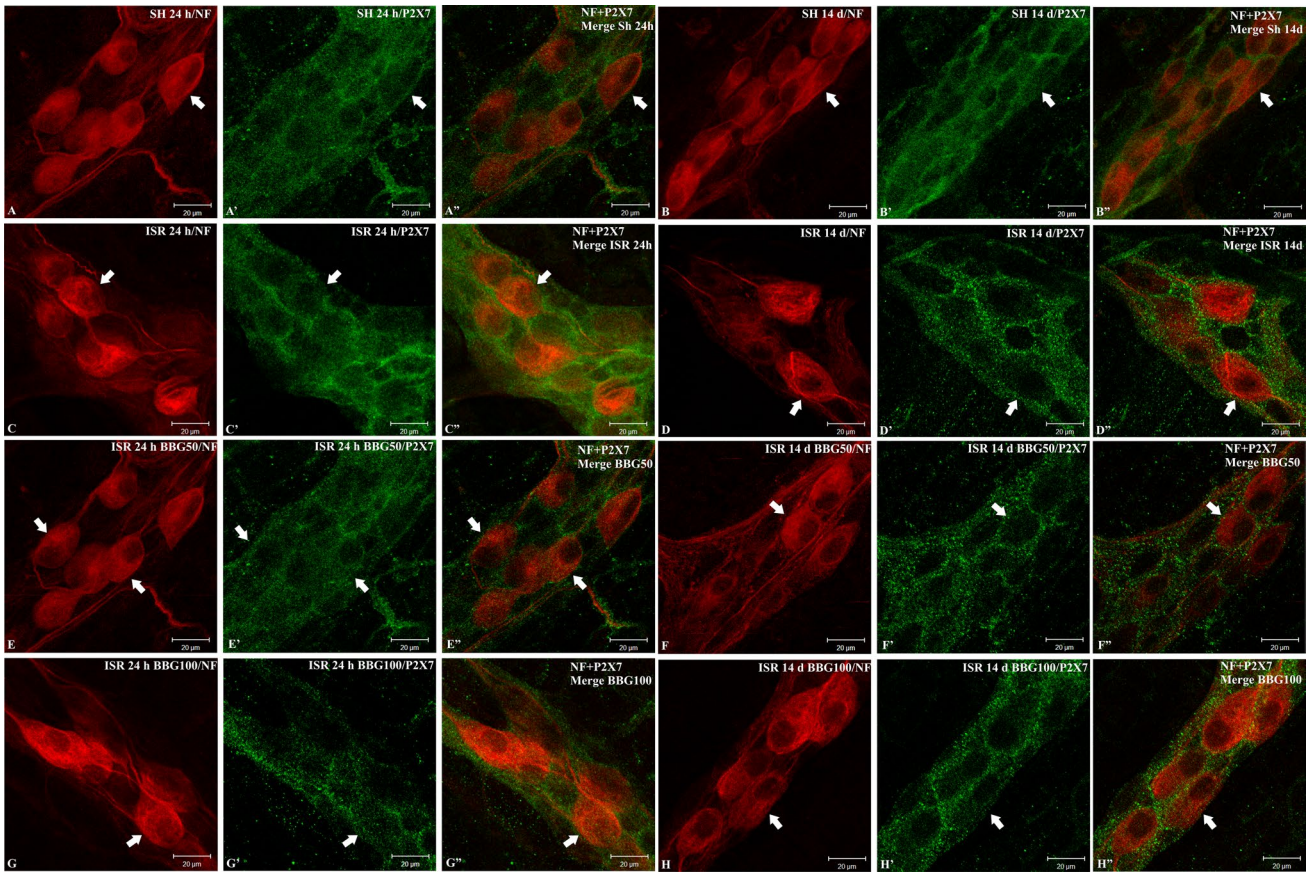

Fig. 2 Double labeling of the P2X7 receptor (P2X7) with neurofilament-200 (NF) in rat ileum myenteric plexus from the SH, ISR, BBG50, and BBG100 groups at 24 h and 14 d. NF (red; **a–h**) colocalized with the P2X7 receptor (green; **a′–h′**). Merge of the P2X7 receptor and NF (**a″–h″**). Single arrows indicate double-labeled neurons. Scale bars, 20 µm

In the circular muscle (CM) layer, the number of neutrophils in the I/R 24-h group increased by 40%, 60%, and 160% compared with that in the sham, BBG50, and BBG100 groups ($P < 0.05$), respectively. In the 14-d group, I/R increased the number of neutrophils by 56% compared with that in the sham, BBG50, and BBG100 groups ($P < 0.001$) (Fig. 4k).

Quantitative Analysis

Double-Labeling Immunoreactivity

Our quantitative analysis showed that the immunoreactivity for nNOS, NF200, and ChAT was 100% colocalized with that for the P2X7 receptor in neurons in the SH, ISR, and BBG groups, indicating that all of these neuronal subtypes also express the P2X7 receptor (Table 2).

Neuronal Density

The neurons per area positive for the P2X7 receptor in the ISR 24-h and ISR 14-d groups decreased by 27% and 22% compared to that in the SH 24-h and SH 14-d groups, respectively ($P < 0.01$). In addition, the numbers of neurons per area positive for the P2X7 receptor in the BBG50 and BBG100 24-h groups increased by 12% and 5.6%, respectively, compared to that in the ISR 24-h group ($P < 0.05$). Moreover, compared to the ISR 14-d group, the BBG50 and BBG100 groups showed increases of 15% and 21%, respectively ($P < 0.01$). The numbers of P2X7 receptor-ir neurons per area did not differ between the SH and BBG 14-d animals (Fig. 5).

The neurons positive for nNOS/cm^2 in the ISR 24-h and ISR 14-d groups decreased by 35% and 45% compared to that in the SH groups ($P < 0.01$). nNOS-ir neurons/cm^2 in the BBG50 and BBG100 24-h groups increased by 22% and

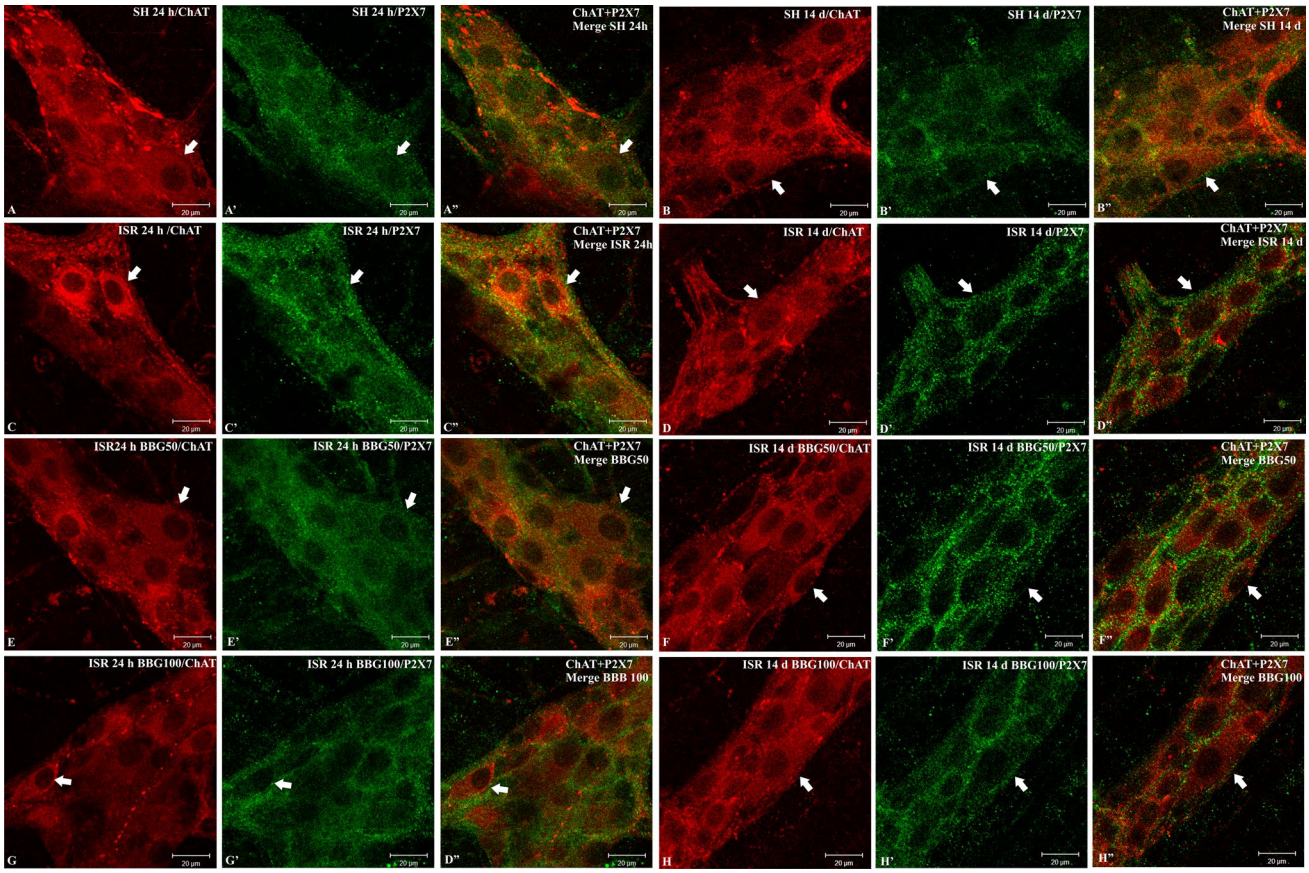

Fig. 3 Double labeling of the P2X7 receptor (P2X7) with choline acetyltransferase (ChAT) in rat ileum myenteric plexus in the SH, ISR, BBG50, and BBG100 groups at 24 h and 14 d. ChAT (red; **a–h**) colocalized with the P2X7 receptor (green; **a′–h′**). Merge of the P2X7 receptor and ChAT (**a″–h″**). Single arrows indicate double-labeled neurons. Scale bars, 20 µm

6.8%, respectively, compared to that in the ISR 24-h group ($P < 0.01$). In addition, compared to the ISR 14-d group, the BBG50 and BBG100 groups showed increases of 20% and 13%, respectively ($P < 0.05$). The density of the nNOS-ir neurons did not differ between the SH 24-h and 14-d groups (Fig. 5).

The NF200-ir neurons/cm^2 in the ISR 24-h and ISR 14-d groups decreased by 39% and 34%, respectively, compared to that in the SH group ($P < 0.001$). Furthermore, the NF200-ir neuronal density in the BBG50 and BBG100 24-h groups increased by 23% and 20%, respectively ($P < 0.001$), compared with that in the ISR 24-h group. Additionally, the NF200-IR density increased by 24% and 7.8% in the BBG50 and BBG100 14-d groups, respectively, compared with that in the ISR 14-d group. No difference in the density of NF200-ir neurons was found between the SH 24-h and 14-d groups (Fig. 5).

Finally, the ChAT-ir neurons per unit area in the ISR 24-h and ISR 14-d groups decreased by 18% and 38% compared to that in the SH group ($P < 0.05$). The ChAT-ir neurons per area in the BBG50 and BBG100 14-d groups increased by 37% and 25%, respectively, compared to that in the ISR 14-d animals ($P < 0.001$). No difference was observed in ChAT-ir neuronal density between the SH 24-h and 14-d groups (Fig. 5).

Morphometric Analysis

The profile area of the nNOS-ir neurons in the ISR 24-h group increased by 16% compared to that in the SH group ($P < 0.01$). In addition, the size in the BBG50 and BBG100 24-h groups was reduced by 19% and 28%, respectively ($P < 0.01$), compared with that in the ISR 24-h group (Fig. 6). Among the 14-d groups, the area of the nNOS-ir neurons increased by 4.7% in the ISR group compared to that in the SH group ($P > 0.05$). Additionally, an increase of 6.2% and a reduction of 4.2% in the BBG50 and BBG100 groups compared to that in the ISR group, respectively ($P < 0.05$) (Fig. 6).

The profile area of the NF200-ir neurons increased by 15% in the ISR 24-h group compared to that in the SH group ($P < 0.05$). Additionally, compared to the ISR group, the BBG50 and BBG100 24-h groups each showed decreases of 17% and 19%, respectively. Among the 14-d groups,

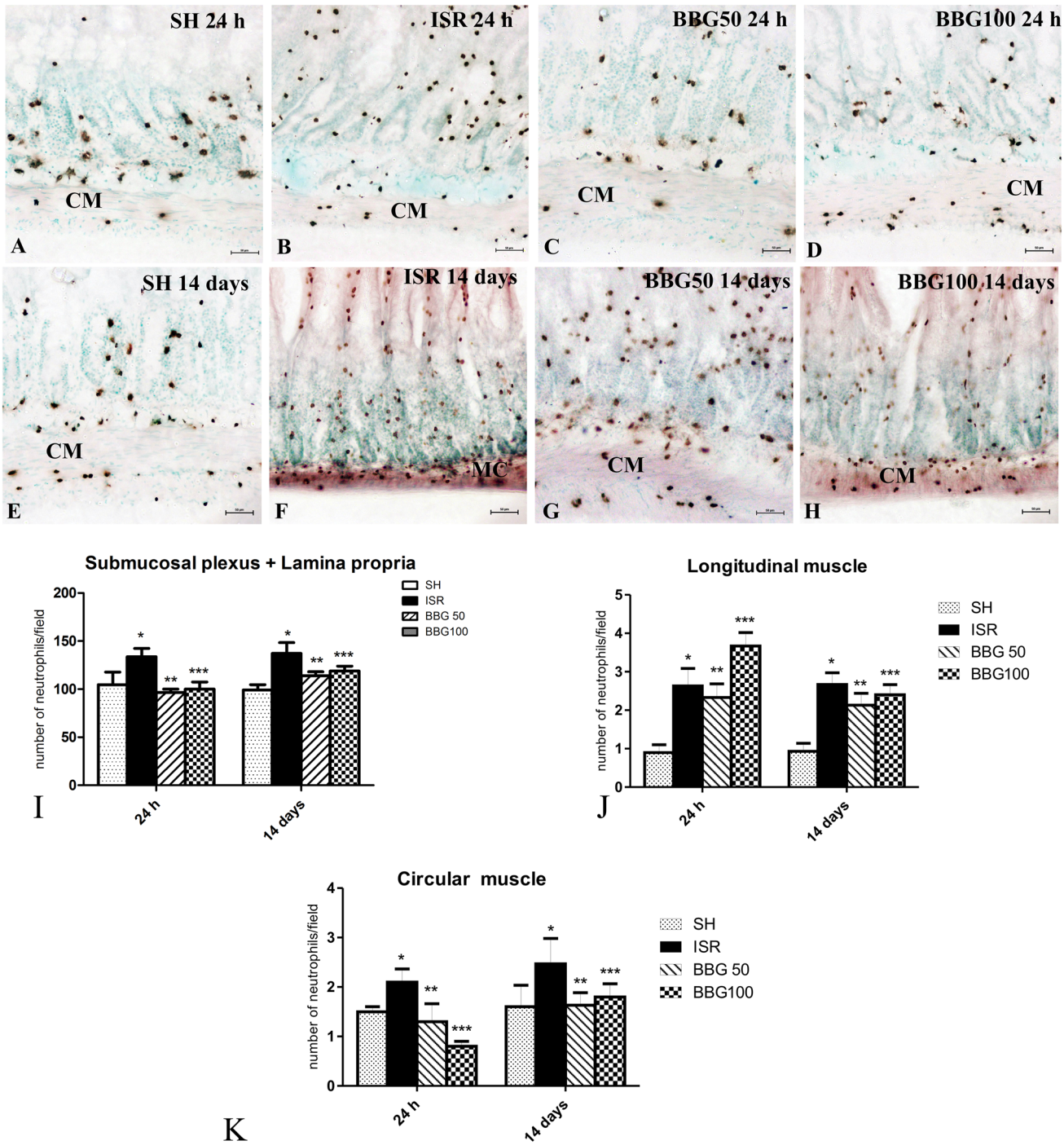

Fig. 4 Neutrophils revealed by myeloperoxidase histochemistry (dark brown cells) in the rat ileum in the SH, ISR, BBG50, and BBG100 24-h (**a**–**d**) and 14-d (**e**–**h**) groups. In the SH groups (**a**, **e**), few MPO-positive cells were present in the intestinal layers. In the ISR 24-h (**b**), ISR 14-d (**f**), BBG50 24-h (**c**), BBG50 14-d, BBG100 24-h (**d**), and BBG100 14-d (**h**) groups, neutrophils were common in the mucosal and muscle layers. *CM* circular muscle. Scale bars, 50 µm. **i** Quantification of neutrophils observed in submucosal plexus + lamina propria, **j** longitudinal muscle, and **k** circular muscle in sections of the ileum from the SH 24-h, ISR 24-h, BBG50 24-h, BBG100 24-h, ISR 14-d, BBG50 14-d, and BBG100 14-d groups. Tissue samples (1 cm) were collected from 5 rats per group either 24 h or 14 d after ischemia. A total of 40 rats were used, and a total of 40 slides were analyzed. The data are presented as the means ± SEM ($n = 5$ per group) and were compared with one-way ANOVA and Tukey's test for multiple comparisons (*ISR group compared to SH group; **BBG50 group compared to ISR; ***BBG100 group compared to ISR group; $P < 0.05$)

Table 2 Double labeling for neurons in the myenteric plexus of the sham, ISR, and BBG groups

Groups	SH 24 h (%)	ISR 24 h (%)	BBG50 24 h (%)	BBG100 24 h (%)	SH 14 d (%)	ISR 14 d (%)	BBG50 14 d (%)	BBG100 14 d (%)
$NOS^+/P2X7^+$	100	100	100	100	100	100	100	100
$P2X7^+/NOS^+$	25 ± 1	22.5 ± 1.4	24.5 ± 1.1	24.5 ± 1.1	26.5 ± 1.6	27.5 ± 3.5	23 ± 1.5	22.5 ± 1.7
$NF200^+/P2X^+$	100	100	100	100	100	100	100	100
$P2X7^+/NF200^+$	31.7 ± 1.9	33 ± 2.4	29.2 ± 0.8	32.7 ± 1.8	33 ± 1.6	28.7 ± 1.0	31.7 ± 1.7	29.2 ± 1.0
$ChAT^+/P2X7^+$	100	100	100	100	100	100	100	100
$P2X7^+/ChAT^+$	45.0 ± 2.0	43.5 ± 1.5	44.0 ± 0.6	45.5 ± 1.6	41.5 ± 1.3	42.0 ± 0.5	41.5 ± 1.3	43.5 ± 0.9

The data are presented as the means ± standard error

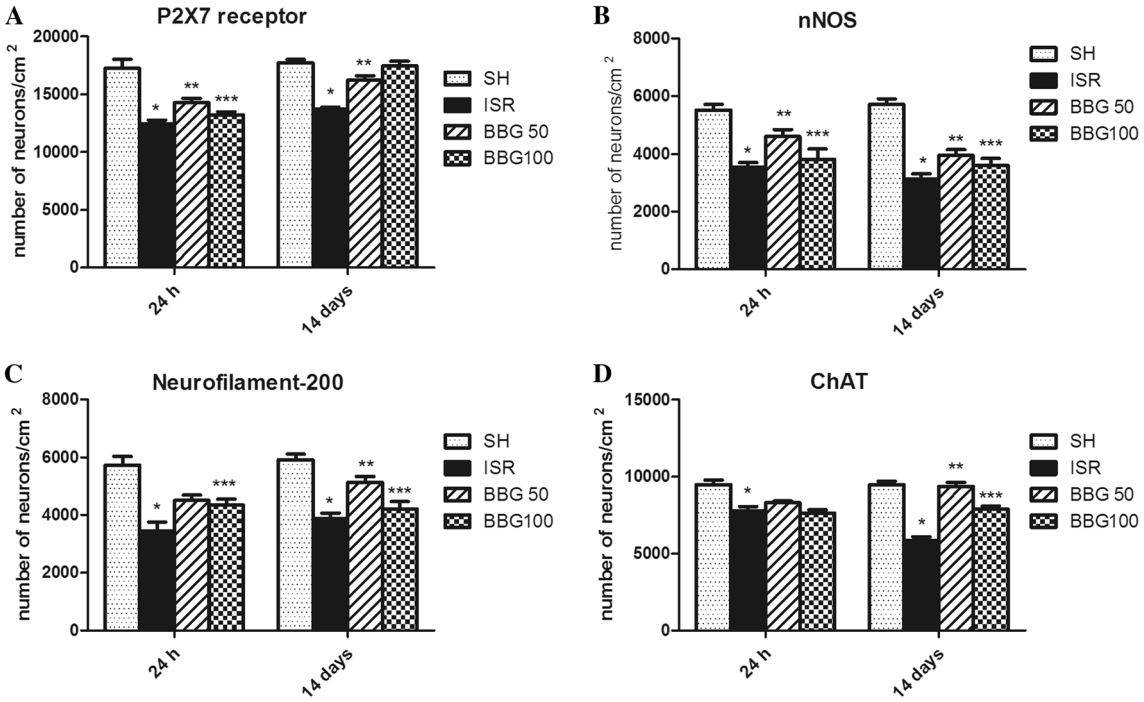

Fig. 5 Neurons per area immunoreactive for the P2X7 receptor (**a**), neuronal nitric oxide synthase (nNOS) (**b**), neurofilament-200 (NF-200) (**c**), and choline acetyltransferase (ChAT) (**d**) in the myenteric plexus of the ileum from the SH, ISR 24-h, BBG50 24-h, BBG100 24-h, ISR 14-d, BBG50 14-d, and BBG100 14-d groups. For each antigen, counting was performed in 40 microscopic fields (0.000379 cm^2) chosen at random in two whole-mount preparations per animal from 5 rats in each group (40 rats total). Each column represents pooled data from five individual immunofluorescence experiments. The data are presented as the means ± SEM ($n = 5$ per group) and were compared with one-way ANOVA and Tukey's test for multiple comparisons (*ISR group compared to SH group; **BBG50 group compared to ISR group; ***BBG100 group compared to ISR group; $*P < 0.01$, **, $***P < 0.05$)

the ISR group showed a 12% decrease in the area of the NF200-ir neurons compared to the SH group ($P < 0.05$), and the BBG100 group showed a 9% increase compared to the ISR group ($P < 0.05$). The profile area of NF200-ir neurons did not differ significantly among the SH, BBG50 24-h, BBG100 24-h, and BBG100 14-d groups (Fig. 6).

The size of ChAT-ir neurons increased by 21.2% in the ISR 24-h group compared to that in the SH group and decreased by 3.7% in the BBG50 and BBG100 groups compared to that in the ISR 24-h group ($P < 0.05$). The ChAT-immunoreactive profile area in the ISR 14-d group increased by 8.4% compared with that in the SH 14-d group but decreased by 10% and 6.7% in the BBG50 and BBG100 groups, respectively, compared to that in the ISR 14-d group ($P < 0.05$) (Fig. 6). No differences in the profile area of the ChAT-ir neurons were detected among the SH, BBG50, and BBG100 14-d groups (Fig. 6).

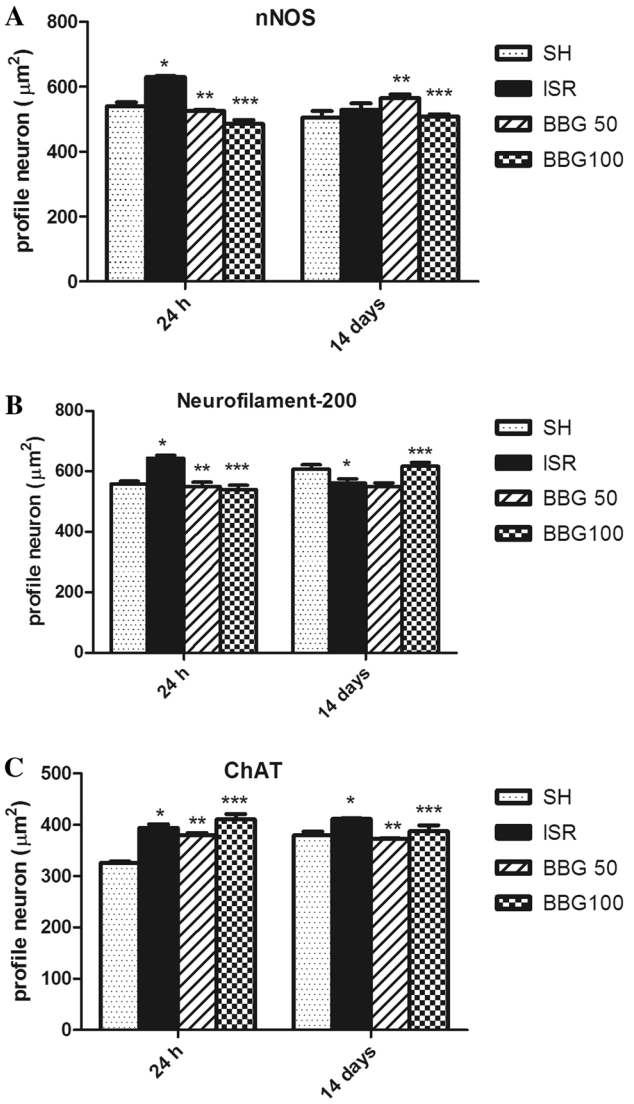

Fig. 6 Size (μm^2) of the profile areas of neurons positive for neuronal nitric oxide synthase (nNOS) (**a**), neurofilament-200 (NF-200) (**b**), and choline acetyltransferase (ChAT) (**c**) in the myenteric plexus of the ileum from the SH 24-h, ISR 24-h, BBG50 24-h, BBG100 24-h, ISR 14-d, BBG50 14-d, and BBG100 14-d groups. The cell profile areas (μm^2) were obtained for 100 randomly selected neurons in two whole-mount preparations per animal per immunoreactivity assay from 5 rats for each group (40 rats total). Each column represents pooled data from 500 neurons. The data are presented as the means ± SEM and were compared with one-way ANOVA and Tukey's test for multiple comparisons (*ISR group compared to SH group; **BBG50 group compared to ISR group; ***BBG100 group compared to ISR group; $P < 0.05$)

Western Blotting Analyses

Protein expression of the P2X7 receptor increased by 17% in the ISR 24-h group compared to that in the SH group ($P > 0.05$) and decreased by 8.5% ($P > 0.05$) and 30% ($P > 0.05$) in the BBG50 and BBG100 24-h groups, respectively, compared to that in the ISR 24-h group (Fig. 7a).

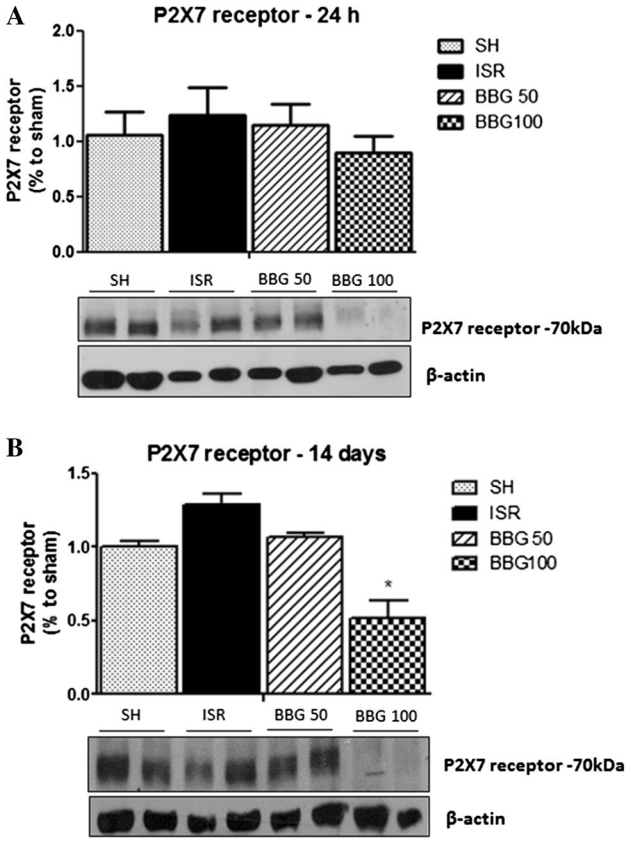

Fig. 7 The protein expression of the P2X7 receptor was assessed in the myenteric plexus + longitudinal muscle ileum from 5 rats per group in the **a** SH 24-h, ISR 24-h, BBG50 24-h, BBG100 24-h and **b** SH 14-d, ISR 14-d, BBG50 14-d, and BBG100 14-d groups. Each column represents pooled data from five individual experiments; a total of 40 rats were used, and 40 experiments were performed to evaluate the expression of the P2X7 receptor. The experiment was repeated twice. The data are presented as the means ± SEM and were compared with one-way ANOVA and Tukey's test for multiple comparisons (*BBG100 group compared to ISR group; $P < 0.05$)

No differences in P2X7 protein expression were observed among the SH, ISR 14-d, and BBG50 14-d groups. Protein expression of the P2X7 receptor decreased by 49% ($P < 0.05$) in the BBG100 14-d group compared to that in the ISR 14-d group (Fig. 7b).

Motility

Spontaneous activity decreased by 18% and 8.8% in the ISR 24-h and ISR 14-d groups compared to that in the SH 24-h and 14-d groups, respectively ($P < 0.05$). In contrast, spontaneous activity increased by 33.8% and 9.9% in the BBG50 24-h and BBG50 14-d groups compared with that in the ISR 24-h and 14-d groups, respectively ($P < 0.05$), and no difference was found between the SH and BBG groups at 14 d (Fig. 8).

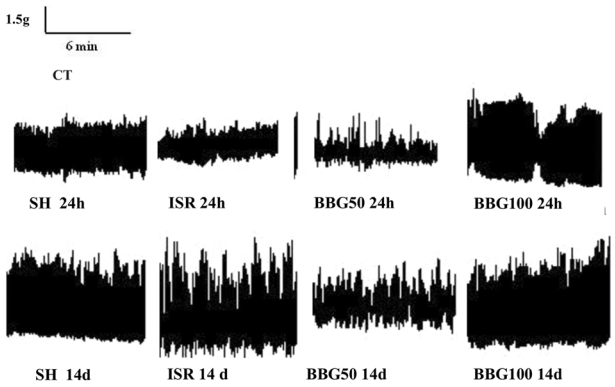

A Tracing of the Spontaneous Activity

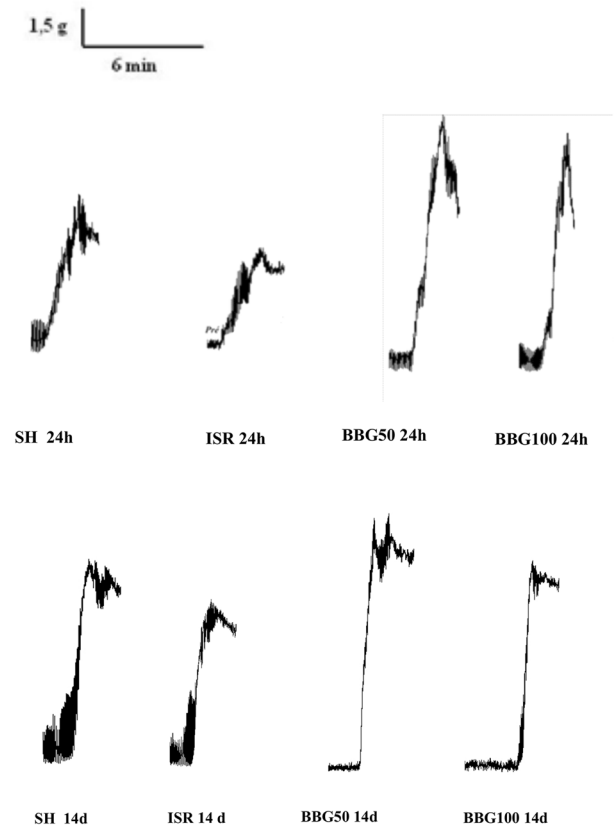

B Tracing of the Carbachol

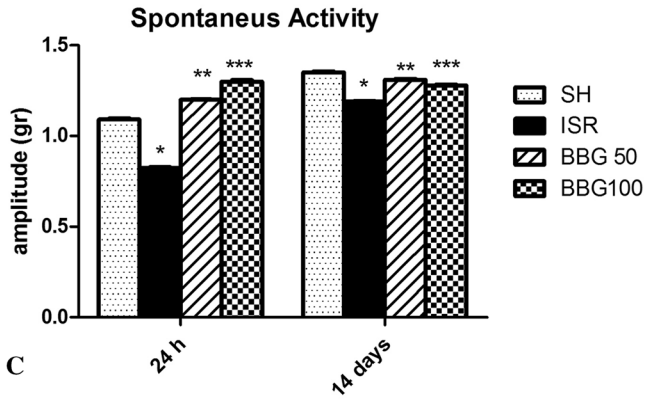

C

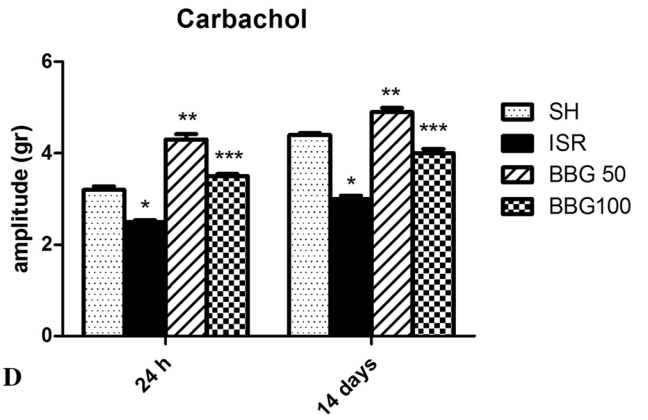

D

Fig. 8 Contractile activity of the ileal segments in the SH 24-h, ISR 24-h, BBG50 24-h, BBG100 24-h, ISR 14-d, BBG50 14-d, and BBG100 14-d groups. **a** Tracings showing spontaneous contractions of the ileum, **b** typical tracings showing the contractions elicited in response to carbachol, **c** quantitative analysis of the changes in the amplitude of the spontaneous activity following ISR and BBG treatments, **d** quantitative analysis of the amplitude in response to carbachol following ISR and BBG treatments. Full-thickness ileal segments from 5 rats in each group were prepared and analyzed. A total of 40 rats were used, and a total of 40 segments were analyzed. Each column represents pooled data from five individual experiments. The data are shown as the means ± SEM and were compared with one-way ANOVA and Tukey's test for multiple comparisons (*ISR group compared to SH group; **BBG50 group compared to ISR group; ***BBG100 group compared to ISR group; $P < 0.05$)

After carbachol treatment, activity decreased by 21.3% and 32% in the ISR 24-h and ISR 14-d groups, respectively, compared to the SH groups ($P < 0.05$). Moreover, activity increased by 41.8% and 28% in the BBG50 and BBG100 24-h groups, respectively, compared to the ISR 24-h group ($P < 0.05$). In addition, compared to the ISR 14-d group, the BBG50 and BBG100 14-d groups showed increases in activity of 38% and 25%, respectively ($P < 0.05$). Finally, no difference in activity was observed among the SH 14-d, BBG50 and BBG100 24-h, and BBG50 14-d groups (Fig. 8).

The addition of SNP to the organ bath inhibited contractions and decreased induced contractions by 22% in the ISR 24-h group compared to those in the SH group ($P < 0.05$). Furthermore, contraction activity increased by 50% and 43% in the BBG50 and BBG100 24-h groups, respectively, compared to that in the ISR 24-h group ($P < 0.05$). Contraction activity decreased by 20% in the ISR 14-d group compared to that in the SH 14-d group and increased by 20% and 11.6% in the BBG50 and BBG100 14-d groups, respectively, compared to that in the ISR 14-d group ($P < 0.05$). No

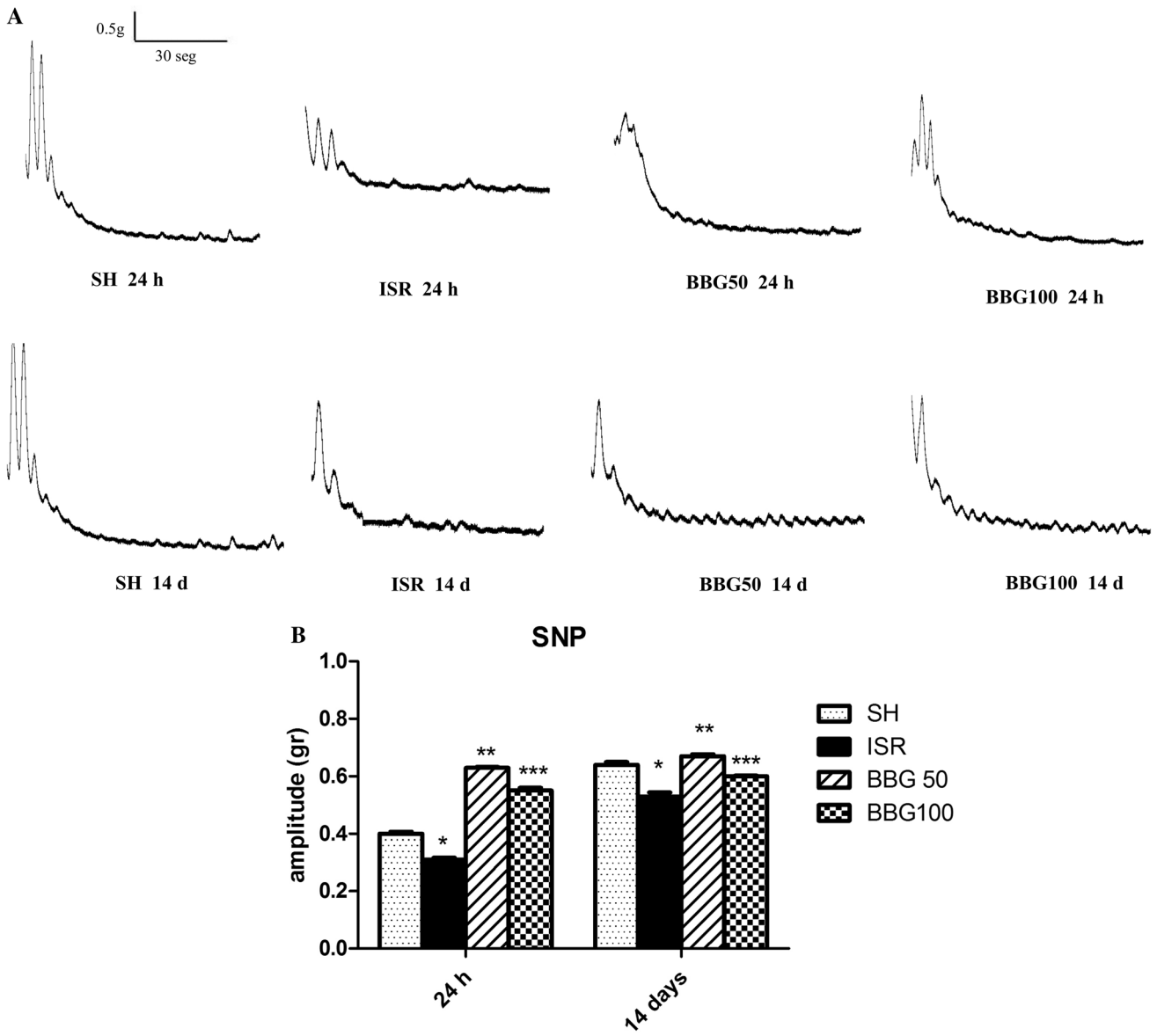

Fig. 9 Contractile activity of the ileal segments in the SH 24-h, ISR 24-h, BBG50 24-h, BBG100 24-h, ISR 14-d, BBG50 14-d, and BBG100 14-d groups. **a** Tracings showing typical the contractions elicited in response to SNP, **b** quantitative analysis of the amplitude in response to SNP following ISR and BBG treatments. Full-thickness ileal segments from 5 rats in each group were prepared and analyzed. A total of 40 rats were used, and a total of 40 segments were analyzed. Each column represents pooled data from five individual experiments. The data are shown as the means ± SEM and were compared with one-way ANOVA and Tukey's test for multiple comparisons (*ISR group compared to SH group; **BBG50 group compared to ISR group; ***BBG100 group compared to ISR group; $P < 0.05$)

difference in activity was detected between the SH 14-d and BBG groups (Fig. 9).

Discussion

Our data demonstrate that subcutaneous injection of BBG reduced the effects of ISR on neuronal density, neuronal area size, number of neutrophils in the intestinal layers, and intestinal motility. In the present study, two doses of BBG were used. The dose of BBG (50 mg/kg) chosen was based on Peng et al. [42]. We also decided to use 100 mg/kg to compare which dose would be more effective in enteric neurons following ISR. The 50 mg/kg dose seemed to be more effective than the 100 mg/kg dose. Furthermore, our results showed that the dose of 100 mg/kg may be toxic to some classes of enteric neurons.

nNOS was used to identify inhibitory motor neurons; ChAT, to identify cholinergic neurons; and NF200, to identify the morphology of Dogiel type II neurons, which are sensory neurons in the rat [1, 2].

The P2X7 receptor antagonist used in this work, BBG, is derived from a food dye and has no known toxicity [37]. Previous work has demonstrated that intravenous injection of BBG significantly decreased spinal cord lesions without obvious toxicity [42], and BBG has been demonstrated to induce a reduction in neuronal death in the hippocampus and activation of astrocytes and microglia in cerebral ischemia [44]. Additionally, Arbeloa et al. [43] treated a rat model of medial cerebral artery occlusion with BBG and observed a 60% reduction in neuronal injury.

The P2X7 receptor is present in myenteric neurons in the ileum [8, 21] and distal colon [33–35]. Our double-immunohistochemistry results demonstrated that in all groups, the P2X7 receptor was present on 100% of the myenteric neurons positive for nNOS, ChAT, and NF200. Myenteric neurons expressing P2X receptors have been demonstrated to be affected by ISR [7–9], indicating that these neurons are activated by extracellular ATP [18]. The P2X7 receptor has been reported to mediate the death of various cells among these neurons and glial cells [19, 20, 32, 46, 47]. For example, Gulbransen et al. [47] demonstrated an increase in P2X7 receptor activation in colitis. Moreover, because of the increase in extracellular ATP levels in colitis, subsequent P2X7 receptor signaling results in increased intracellular Ca^{2+} influx from the extracellular environment through this ion channel, causing neuronal death [31]. Roberts et al. [48] found that inflammation can lead to the release of purines, which can activate and modulate purinergic signaling, resulting in the loss of enteric neurons via the P2X7 receptor.

Purines and pyrimidines are liberated actively or passively from cells under normal or injury conditions [20]. In certain injury conditions, such as inflammation, ATP levels in the extracellular space may increase drastically [49]. In ischemic stress, ATP exerts excitotoxic effects mediated by P2 receptors in several cell types [19]. Additionally, the authors have described that the P2X7 receptor initiates apoptosis in several cell types [50, 51]. The P2X7 receptor forms a pore in the cell membrane in response to a stimulus and can regulate cell permeability and the release of cytokines as well as trigger apoptosis [20].

Changes in the numbers of enteric neurons per unit area have been investigated in protocols such as malnutrition/renutrition [33, 52–54]. Obese *ob*/*ob* mice exhibit fewer nNOS-ir and ChAT-ir neurons per unit area [55, 56]. Additionally, after 60 min of ischemia of the ileal arteries in guinea pigs, Rivera et al. [57] observed a decrease in the number of nNOS-positive neurons. Our results showed that the numbers of immunoreactive neurons per unit area for the P2X7 receptor, nNOS, NF200, and ChAT were lower in the ISR groups; however, after treatment with BBG at either concentration, the numbers of these immunoreactive neurons per unit area recovered within the 24-h and 14-d periods. Previous studies demonstrated that activation of the P2X7 receptor leads to the influx of intracellular Ca^{2+}, which activates apoptotic pathways [19, 20, 58]. In the present study, treatment with the P2X7 receptor antagonist recovered the myenteric neurons and may have blocked activation death pathways.

Previous work has also verified that after mechanical injury, spinal cord neurons can be reestablished with the use of BBG, corroborating the participation of the P2X7 receptor in neuronal death [42]. Additionally, the P2X7 receptor antagonist BBG has been demonstrated to reduce the effect of cerebral ischemia on neurons [43, 44].

The area of the myenteric neuronal profile has been extensively studied in various neurons in female and male obese mice [55, 56], and inflammation causes a decrease in the neuronal profile of myenteric neurons [34]. Rivera et al. [57] described morphological changes in the myenteric plexus after ISR. After measuring the area of the profile, we observed an increase in the nNOS- and ChAT-ir profiles and a reduction in the NF200-ir profile 14 d after ischemia. However, the profile area of these neurons was recovered in the animals treated with BBG.

Neutrophils have phagocytic activity and are the major cellular elements in many forms of inflammation. Kalff et al. [59] showed that leukocyte extravasation was present in the muscle layer when the intestine was manipulated. During intestinal reperfusion, neutrophils rapidly invade the external musculature and secrete molecules, including MPO [60, 61], which has also been verified in the ileum musculature following ISR [45]. In the present work, neutrophils were counted in the SP + LP layers and the longitudinal and circular muscles. Neutrophils were observed in these regions in all groups studied. However, an increase in neutrophils

was observed in the ISR groups, and BBG treatment reduced their number. The presence of neutrophils in the small intestine of the rat and mouse after ISR has been observed previously [45, 62].

Although more neutrophils were detected in the BBG-treated groups than in the SHs, fewer neutrophils were observed in the BBG-treated groups than in the ISR groups not treated with BBG, suggesting that BBG not only acts to protect the enteric neurons but also reduces the effects of ischemia on the intestinal wall. The reduction in the number of neutrophils treated with BBG suggests that the P2X7 receptor plays a role in inflammation [63]. In a previous study, treatment with BBG was shown to reduce neutrophil infiltration after spinal cord injury [42].

The MPO reaction has been previously demonstrated in inflamed tissues [64]. Additionally, purinergic signaling has been suggested to modulate neutrophil chemotaxis [65]. Furthermore, P2X7 receptor activation can lead to the regulation of cytokine responses in inflammatory processes [65], and the P2X7 receptor is a key factor in inflammasome activation in the production of interleukin (IL)-1β and IL-18 [66, 67].

ISR is known to cause changes in bowel motility, with some studies showing a delay in gastrointestinal transit and the responses to pharmacological and electrical stimuli in ischemia protocols [62, 68, 69]. In our study, changes in intestinal motor activity were demonstrated in a model of intestinal ischemia with different reperfusion periods. In the ISR 24-h group, there was a decrease in spontaneous intestinal activity and a recovery with BBG treatment. Decreases in intestinal contractility have previously been reported in ischemia protocols [45, 69, 70].

During ISR, nitric oxide (NO) is thought to be involved in the relaxation of the intestinal musculature along with the regulation of nonadrenergic and noncholinergic contractions of neurons, and ISR induces NO production, thereby altering intestinal motility [71].

An NO donor, SNP, has been shown to inhibit spontaneous contractions [62, 69, 72]. To analyze the effect of NO on spontaneous activity, a single dose of SNP was used. Our results demonstrated a decrease in relaxation in the 24-h ISR group; however, BBG restored bowel relaxation. A decrease in the relaxation of the ileal segments of rats subjected to superior mesenteric artery ischemia with 24 h of reperfusion has also been reported with the use of indomethacin to induce bowel relaxation [73]. Additionally, the upregulation of inducible NOS (iNOS)-immunoreactive neurons following ISR has been demonstrated [74]. Moreover, Toll-like receptor 4 (TLR4) modulates motility and survival of distal colon enteric neurons [75]. TLR4 knockout mice showed reduced nNOS neurons in the ileum myenteric plexus and a decrease in the amplitude of relaxation with the addition of a selective antagonist of the P2X7 receptor [76].

Agonists of cholinergic muscarinic receptors, such as carbachol, have been used to study intestinal contractility, resulting in a decrease in spontaneous activity in protocols such as aging [77]. Furthermore, a reduction in the contraction amplitude in response to carbachol in the ileum of mice with ISR has been verified [45]. Our results agreed with the literature and demonstrated that the maximum peaks of contraction reached with carbachol treatment were lower in the 24-h ISR group than in the SH group. In the BBG100 24-h and 14-d groups, the contractility in response to carbachol returned to normal levels. Similar data have been reported on reductions in the acetylcholine response in an ISR model [73].

Our work demonstrated that in a model of ISR treated with the selective antagonist BBG, the effects of ischemia on neurons were prevented or diminished, thus demonstrating the probable participation of the P2X7 receptor in the neuronal changes induced by ischemia. In addition, the effects of ischemia on the ENS can result in gastrointestinal dysfunction, such as decreased intestinal motility, but treatment with BBG was observed to prevent dysmotility. Thus, these results demonstrate that the P2X7 receptor may be an important target in the therapeutic strategy for ISR injury.

Acknowledgments We would like to thank Rosana Prisco for the statistical analysis. These studies were supported by São Paulo Foundation Research (FAPESP Grants Nos. 2010/10510-8, 2012/00259-1, 2014/25927-2) and CAPES.

Author's contribution KP performed the experiments and analyzed the results. CEM helped with the immunohistochemistry study and ISR surgery. WTL helped edit the manuscript. MLBC helped in the Western blotting study. PC planned experiments, analyzed the results, and wrote and edited the manuscript.

Compliance with ethical standards

Conflict of interest The authors declare that they have no conflict of interest.

References

1. Furness JB. *The enteric nervous system*. Oxford: Blackwell; 2006.
2. Furness JB. The enteric nervous system and neurogastroenterology. *Nat Rev Gastroenterol Hepatol*. 2012;9:286–294.
3. Guan Y, Worrell RT, Pritts TA, Montrose MH. Intestinal ischemia–reperfusion injury: reversible and irreversible damage imaged in vivo. *Am J Physiol Gastrointest Liver Physiol*. 2009;297:187–196.
4. Haglund U, Bergqvist D. Intestinal ischemia—the basics. *Langenbeck's Arch Surg*. 1999;384:233–238.
5. Oldenburg A, Lau LL, Rodenberg TJ, Edmonds HJ, Burger CD. Acute mesenteric ischemia. A clinical review. *Arc Intern Med*. 2004;164:1054–1061.
6. Lindestrom L, Ekblad E. Structural and neuronal changes in rat ileum after ischemia with reperfusion. *Dig Dis Sci*. 2004;49:1212–1222. https://doi.org/10.1023/B:DDAS.0000037815.63547.08.

7. Paulino AS, Palombit K, Cavriani G, et al. Effects of ischemia and reperfusion on $P2X_2$ receptor expressing neurons of the rat ileum enteric nervous system. *Dig Dis Sci*. 2011;56:2262–2277. https://doi.org/10.1007/s10620-011-1588-z.
8. Palombit K, Mendes CE, Tavares-De-Lima W, Castelucci P. Effects of ischemia and reperfusion on subpopulations of rat enteric neurons expressing the P2X7 receptor. *Dig Dis Sci*. 2013;58:3429–3439. https://doi.org/10.1007/s10620-013-2847-y.
9. Marosti AR, da Silva MV, Palombit K, Mendes CE, Tavares-de-Lima W, Castelucci P. Differential effects of intestinal ischemia and reperfusion in rat enteric neurons and glial cells expressing P2X2 receptors. *Histol Histopathol*. 2015;30:489–501.
10. Mendes CE, Palombit K, Vieira C, Silva I, Correia-de-Sá P, Castelucci P. The effect of ischemia and reperfusion on enteric glial cells and contractile activity in the ileum. *Dig Dis Sci*. 2015;60:2677–2689. https://doi.org/10.1007/s10620-015-3663-3.
11. Ralevic V, Burnstock G. Receptors for purines and pyrimidines. *Pharmacol Rev*. 1998;50:413–492.
12. Burnstock G. A basis for distinguishing two types of purinergic receptor. In: Straub RW, Bolis L, eds. *Cell membrane receptors for drugs and hormones. A multidisciplinary approach*. New York: Raven Press; 1978:107–118.
13. North RA, Surprenant A. Pharmacology of cloned P2X receptors. *Annu Rev Pharmacol Toxicol*. 2000;40:563–580.
14. North A. Molecular physiology of P2X receptors. *Physiol Rev*. 2002;82:1013–1067.
15. Burnstock G, Kennedy C. Is there a basis for distinguishing two types of P2-purinoceptor? *Gen Pharmacol*. 1985;16:433–440.
16. Galligan JJ. Ligand-gated ion channels in the enteric nervous system. *Neurogastroenterol Motil*. 2002;14:611–623.
17. Abbrachio MP, Burnstock G, Verkhratsky A, Zimmermann H. Purinergic signaling in the nervous system: an overview. *Trends Neurosci*. 2009;32:19–29.
18. Burnstock G. Purinergic signalling in the gastrointestinal tract and related organs in health and disease. *Purinergic Signal*. 2014;10:3–50.
19. Franke H, Krüel U, Illes P. P2 receptors and neuronal injury. *Euro J Physiol*. 2006;452:622–644.
20. Sperlágh B, Illes P. P2X7 receptor, an emerging target in central nervous system diseases. *Trends Pharmacol Sci*. 2014;35:537–547.
21. Vulchanova L, Arvidsson U, Riedl M, et al. Differential distribution of two ATP-gated ion channels (P2X receptors) determined by immunohistochemistry. *Proc Natl Acad Sci*. 1996;93:8063–8067.
22. Hu HZ, Gao N, Lin Z, et al. $P2X_7$ receptors in the enteric nervous system of guinea-pig small intestine. *J Comp Neurol*. 2001;440:299–310.
23. Castelucci P, Robbins HL, Poole DP, Furness JB. The distribution of purine $P2X_2$ receptors in the guinea pig enteric nervous system. *Histochem Cell Biol*. 2002;117:415–422.
24. Poole DP, Castelucci P, Robbins HL, Chiocchetti R, Furness JB. The distribution of $P2X_3$ purine receptor subunits in the guinea-pig enteric nervous system. *Auton Neurosci*. 2002;101:39–47.
25. Van Nassauw L, Brouns I, Adraensen D, Burnstock G, Timmermans JP. Neurochemical identification of enteric neurons expressing P2X(3) receptors in the guinea-pig ileum. *Histochem Cell Biol*. 2002;118:193–203.
26. Xiang Z, Burnstock G. Distribution of $P2Y_2$ receptors in the guinea pig enteric nervous system and its coexistence with $P2X_2$ and $P2X_3$ receptors, neuropeptide Y, nitric oxide synthase and calretinin. *Histochem Cell Biol*. 2005;124:379–390.
27. Xiang Z, Burnstock G. $P2X_2$ and $P2X_3$ purinoceptors in the rat enteric nervous system. *Histochem Cell Biol*. 2004;12:169–179.
28. Yu Q, Zhao Z, Sun J, Guo W, Fu J, Burnstock G. Expression of $P2X_6$ receptors in the enteric nervous system of the rat gastrointestinal tract. *Histochem Cell Biol*. 2010;133:177–188.
29. Giaroni C, Knight GE, Ruan H-Z, et al. P2 receptors in the murine gastrointestinal tract. *Neuropharmacology*. 2002;43:1313–1323.
30. Ruan HZ, Burnstock G. The distribution of P2X5 purinergic receptors in the enteric nervous system of mouse. *Cell Tissue Res*. 2005;319:191–200.
31. Sperlágh B, Vizi ES, Wirkner K, Illes P. P2X7 receptors in the nervous system. *Prog Neurobiol*. 2006;78:327–346.
32. Burnstock G. An introduction to the roles of purinergic signalling in neurodegeneration, neuroprotection and neuroregeneration. *Neuropharmacology*. 2016;104:4–17.
33. Girotti PA, Misawa R, Palombit K, Mendes CE, Bittencourt JC, Castelucci P. Differential effects of undernourishment on the differentiation and maturation of rat enteric neurons. *Cell Tissue Res*. 2013;353:367–380.
34. Da Silva MV, Marosti AR, Mendes CE, Palombit K, Castelucci P. Differential effects of experimental ulcerative colitis on P2X7 receptor expression in enteric neurons. *Histochem Cell Biol*. 2015;143:171–184.
35. Da Silva MV, Marosti AR, Mendes CE, Palombit K, Castelucci P. Submucosal neurons and enteric glial cells expressing the P2X7 receptor in rat experimental colitis. *Acta Histochem*. 2017;119:481–494.
36. Wang X, Arcuino G, Takano T, et al. P2X7 receptor inhibition improves recovery after spinal cord injury. *Nat Med*. 2004;10:821–827.
37. Volonté C, Apolloni S, Skaper SD, Burnstock G. $P2X_7$ receptors, channels, pores and more. *CNS Neurol Disord Drug Targets*. 2012;11:705–721.
38. Jiang LH, Mackenzie AB, North RA, Surprenant A. Brilliant Blue G selectively blocks ATP-gated rat P2X7 receptors. *Mol Pharmacol*. 2000;58:82–88.
39. Remy M, Thaler S, Schumann RG, et al. An in vivo evaluation of Brilliant Blue G in animals and humans. *Br J Ophtalmol*. 2008;92:1142–1147.
40. Ryu JK, Mclarnon JG. Block of purinergic P2X(7) receptor is neuroprotective in an animal model of Alzheimer's disease. *Neuroreport*. 2008;19:1715–1719.
41. Díaz-Hernández M, Díez-Zaera M, Sánchez-Nogueiro J, et al. Altered P2X7-receptor level and function in mouse models of Huntington's disease and therapeutic efficacy of antagonist administration. *FASEB J*. 2009;23:1893–1906.
42. Peng W, Cotrina ML, Han X, et al. Systemic administration of an antagonist of the ATP-sensitive receptor P2X7 improves recovery after spinal cord injury. *Proc Natl Acad Sci*. 2009;106:12489–12493.
43. Arbeloa J, Pérez-Samartín A, Gottlieb M, Matute C. P2X7 receptor blockade prevents ATP excitotoxicity in neurons and reduces brain damage after ischemia. *Neurobiol Dis*. 2012;45:954–961.
44. Chu K, Yin B, Wang J, et al. Inhibition of P2X7 receptor ameliorates transient global cerebral ischemia/reperfusion injury via modulating inflammatory responses in the rat hippocampus. *J. Neuroinflamm*. 2012;18:69–75.
45. Rivera LR, Thacker M, Castelucci P, Poole DP, Frugier T, Furness JB. Knock out of neuronal nitric oxide synthase exacerbates intestinal ischemia/reperfusion injury in mice. *Cell Tissue Res*. 2012;349:565–576.
46. Franke H, Illes P. Involvement of P2 receptors in the growth and survival of neurons in the CNS. *Pharmacol Ther*. 2006;109:297–324.
47. Gulbransen BD, Bashashati M, Hirota SA, et al. Activation of neuronal $P2X_7$ receptor–pannexin-1 mediates death of enteric neurons during colitis. *Nat Med*. 2012;18:600–604.
48. Roberts JA, Lukewich MK, Sharkey KA, Furness JB, Mawe GM, Lomax AE. The roles of purinergic signaling during gastrointestinal inflammation. *Curr Opin Pharmacol*. 2012;12:659–666.

49. Antonioli L, Giron MC, Colucci R, et al. The role of purinergic pathways in the pathophysiology of gut diseases, pharmacological modulation and potential therapeutic applications. *Pharmacol Ther*. 2013;139:157–188.
50. Coutinho-Silva R, Persechini PM, Bisaggio RD, et al. P2Z/P2X7 receptor-dependent apoptosis of dendritic cells. *Am J Physiol*. 1999;276:C1139–C1147.
51. Slater M, Barden JA, Murphy CR. The purinergic calcium channels P2X1,2,5,7 are down-regulated while P2X3,4,6 are up-regulated during apoptosis in the ageing rat prostate. *Histochem J*. 2000;32:571–580.
52. Castelucci P, De Souza RR, De Angelis RC, Furness JB, Liberti EA. Effects of pre- and postnatal protein deprivation and postnatal re-feeding on myenteric neurons of the rat large intestine: a quantitative morphological study. *Cell Tissue Res*. 2002;310:1–7.
53. Gomes OA, Castelucci P, Fontes RBV, Liberti EA. Effects of pre- and postnatal protein and postnatal re-feeding on myenteric neurons of the rat small intestine, a quantitative morphological study. *Auton Neurosci*. 2006;126:277–284.
54. Misawa R, Girotti PA, Mizuno MS, Liberti EA, Furness JB, Castelucci P. Effects of protein deprivation and re-feeding on $P2X_2$ receptors in enteric neurons. *World J Gastroenterol*. 2010;16:3651–3663.
55. Mizuno MS, Crisma AR, Borelli P, Castelucci P. Expression of the $P2X_2$ receptor in different classes of ileum myenteric neurons in the female obese ob/ob mouse. *World J Gastroenterol*. 2012;18:4693–4703.
56. Mizuno MS, Crisma AR, Borelli P, Schäfer BT, Silveira MP, Castelucci P. Distribution of the $P2X_2$ receptor and chemical coding in ileal enteric neurons of obese male mice (ob/ob). *World J Gastroenterol*. 2014;20:13911–13919.
57. Rivera LR, Thacker M, Castelucci P, Bron R, Furness JB. The reactions of specific neuron types to intestinal ischemia in the guinea pig enteric nervous system. *Acta Neuropathol*. 2009;118:261–270.
58. Fellin T, Pozzan T, Carmignoto G. Purinergic receptors mediate two distinct glutamate release pathways in hippocampal astrocytes. *J Biol Chem*. 2006;281:4274–4284.
59. Kalff JC, Schraut WH, Simmons RL, Bauer AJ. Surgical manipulation of the gut elicits an intestinal muscularis inflammatory response resulting in postsurgical ileus. *Ann Surg*. 1998;228:652–663.
60. Hierholzer C, Kalff JC, Audolfsson G, et al. Molecular and functional contractile sequelae of rat intestinal ischemia/reperfusion injury. *Transplantation*. 1999;68:1244–1254.
61. Massberg S, Messmer K. The nature of ischemia/reperfusion injury. *Transplant Proc*. 1998;30:4217–4223.
62. Filpa V, Carpanese E, Marchet S, et al. Nitric oxide regulates homeoprotein OTX1 and OTX2 expression in the rat myenteric plexus after intestinal ischemia–reperfusion injury. *Am J Physiol Gastrointest Liver Physiol*. 2017;312:G374–G389.
63. Pedata F, Dettori I, Coppi E, Melani A, Tweardy DJ, Bauer AJ. Purinergic signalling in brain ischemia. *Neuropharmacology*. 2016;104:105–130.
64. Morris GP, Beck PL, Herridge MS, et al. Hapten-induced model of chronic inflammation and ulceration in the rat colon. *Gastroenterology*. 1989;96:795–803.
65. Corriden R, Chen Y, Inoue Y, et al. GEcto-nucleoside triphosphate diphosphohydrolase 1 (E-NTPDase1/CD39) regulates neutrophil chemotaxis by hydrolyzing released ATP to adenosine. *J Biol Chem*. 2008;283:28480–28486.
66. Di Virgilio F. Liaisons dangereuses, P2X(7) and the inflammasome. *Trends Pharmacol Sci*. 2007;28:465–472.
67. Csölle C, Sperlágh B. Peripheral origin of IL-1beta production in the rodent hippocampus under in vivo systemic bacterial lipopolysaccharide (LPS) challenge and its regulation by P2X(7) receptors. *J Neuroimmunol*. 2010;219:38–46.
68. Hassoun HT, Weisbrodt NW, Mercer DW, Kozar RA, Mooy FG, Moore FA. Inducible nitric oxide synthase mediates gut ischemia/reperfusion-induced ileus only after severe insults. *J Surg Res*. 2001;97:150–154.
69. Takahashi A, Tomomasa TH, Kaneko H, et al. Intestinal motility in an in vivo rat model of intestinal ischemia–reperfusion with special reference to the effects of nitric oxide on the motility changes. *J Pediatr Gastroenterol Nutr*. 2001;33:283–288.
70. Taha MO, Miranda-Ferreira R, Paez RP, et al. Role of L-arginine, a substrate of nitric oxide biosynthesis, on intestinal ischemia–reperfusion in rabbits. *Transplant Proc*. 2010;42:448–450.
71. Caplan MS, Hedlund E, Hill N, Mackendrick W. The role of endogenous nitric oxide and platelet-activating factor in hypoxia-induced intestinal injury in rats. *Gastroenteroly*. 1994;106:346–352.
72. Ragy M, Elbassuoni E. The role of nitric oxide and L-type calcium channel blocker in the contractility of rabbit ileum in vitro. *J Physiol Biochem*. 2012;68:521–528.
73. Ballabeni V, Barocelli E, Bertoni S, Impicciatore M. Alterations of intestinal motor responsiveness in a model of mild mesenteric ischemia/reperfusion in rats. *Life Sci*. 2002;71:2025–2035.
74. Giaroni C, Marchet S, Carpanese E, et al. Role of neuronal and inducible nitric oxide synthases in the guinea pig ileum myenteric plexus during in vitro ischemia and reperfusion. *Neurogastroenterol Motil*. 2013;25:e114–e126.
75. Anitha M, Vijay-Kumar M, Sitaraman SV, Gewirtz AT, Srinivasan S. Gut microbial products regulate murine gastrointestinal motility via Toll-like receptor 4 signaling. *Gastroenterology*. 2012;143:1006.e4–1016.e4.
76. Caputi V, Marsilio I, Cerantola S, et al. Toll-like receptor 4 modulates small intestine neuromuscular function through nitrergic and purinergic pathways. *Front Pharmacol*. 2017;8:350. https://doi.org/10.3389/fphar.2017.00350.
77. Tran L, Greenwood-Van Meerveld B. In a non-human primate model, aging disrupts the neural control of intestinal smooth muscle contractility in a region-specific manner. *Neurogastroenterol Motil*. 2014;26:410–418.